Pairing in the two-dimensional Hubbard model: An exact diagonalization study

H. Q. Lin* and J. E. Hirsch
Department of Physics, University of California, San Diego, La Jolla, California 92093

D. J. Scalapino
Department of Physics, University of California, Santa Barbara, Santa Barbara, California 93106
(Received 24 August 1987)

We have studied the pair susceptibilities for all possible pair wave functions that fit on a two-dimensional (2D) eight-site Hubbard cluster by exact diagonalization of the Hamiltonian. Band fillings corresponding to four and six electrons were studied (two or four holes in the half-filled band) for a wide range of Hubbard interaction strengths and temperatures. Our results show that all pairing susceptibilities are suppressed by the Hubbard repulsion. We have also carried out perturbation-theory calculations which show that the leading-order U^2 contributions to the d-wave pair susceptibility suppresses d-wave pairing over a significant temperature range. These results are consistent with recent Monte Carlo results and provide further evidence suggesting that the 2D Hubbard model does not exhibit superconductivity.

I. INTRODUCTION

The question of whether the two-dimensional repulsive Hubbard model exhibits superconductivity is of great current interest, in view of the fact that it is one of the possible models to describe the recently discovered high-T_c oxide superconductors.[1] Although a variety of approximate calculations predict superconductivity in this model,[1-11] the need for calculations that do not rely on uncontrolled approximations clearly exists. In this paper we discuss results obtained from an exact calculation on eight-site clusters for a variety of interaction strengths and temperatures and two values of the band filling: $\rho=0.5$ and 0.75, corresponding to four and six electrons (i.e., a half-filled band with two and four holes, respectively). In another paper, results of Monte Carlo simulations of the two-dimensional Hubbard model are discussed.[12] The simulation approach does not reach as low a temperature or as large an interaction strength as the present study but applies to considerably larger clusters. Thus these calculations are complementary.

Most theoretical approaches have suggested extended s-wave or d-wave singlet pairing for the repulsive Hubbard model, involving pairs formed by nearest-neighbor electrons of opposite spins. In the present calculation we have considered all possible pairing of electrons that fit onto an eight-site lattice. We thus obtain an 8×8 pairing matrix, and the eigenvector associated with the largest eigenvalue of this matrix describes the most favorable pairing state. We find that usually the most favorable pairing involves a mixture of states with d- and s-wave symmetry[13] and that contributions from further than nearest-neighbor pairs can be significant. Most importantly, however, we find that the susceptibility associated with this and all other pairing is *suppressed* by the Hubbard interaction.

To shed further light on this question, we compute in perturbation theory the leading (U^2) contribution to the d-wave pair susceptibility, which was found to be the most favorable state near the half-filled band case in previous calculations.[3,11] We find the leading U^2 contribution to *suppress* d-wave pairing over a significant temperature range, consistent with our numerical results on small clusters. The results discussed here, together with Monte Carlo simulation results of Ref. 12, suggest that the two-dimensional repulsive Hubbard model does not exhibit superconductivity.

In Sec. II we describe the cluster formalism. We present our numerical results in Sec. III, perturbation theory results in Sec. IV, and conclude with a short discussion in Sec. V.

II. CLUSTER FORMALISM

The Hubbard model on a two-dimensional lattice is defined by the Hamiltonian

$$H=\sum_{i,j,\sigma} t_{ij}C_{i\sigma}^{\dagger}C_{j\sigma}+U\sum_{i} n_{i\uparrow}n_{i\downarrow}-\mu\sum_{i,\sigma} n_{i\sigma} \tag{1}$$

$$=\sum_{\mathbf{k},\sigma}\varepsilon_{\mathbf{k}}C_{\mathbf{k}\sigma}^{\dagger}C_{\mathbf{k}\sigma}+\frac{U}{N}\sum_{\mathbf{k}_1,\mathbf{k}_2,\mathbf{k}_3} C_{\mathbf{k}_1\uparrow}^{\dagger}C_{\mathbf{k}_2\uparrow}C_{\mathbf{k}_3\downarrow}^{\dagger}C_{\mathbf{k}_1-\mathbf{k}_3-\mathbf{k}_2\downarrow}\ , \tag{2}$$

where

$$\varepsilon_{\mathbf{k}}=-2t_x\cos k_x-2t_y\cos k_y+4t_2\cos k_x\cos k_y-\mu\ . \tag{3}$$

In Eq. (1), $C_{i\sigma}^{\dagger}$ ($C_{i\sigma}$) is the creation (annihilation) operator for spin $\sigma=\uparrow\downarrow$ at site i, and $C_{\mathbf{k}\sigma}^{\dagger}$ ($C_{\mathbf{k}\sigma}$) is its Fourier component. μ is the chemical potential, and t_{ij} is the hopping term. Here $t_{ij}=t_x$ for (i,j) nearest neighbors in the x direction, $t_{ij}=t_y$ for (i,j) nearest neighbors in the y direction, and $t_{ij}=t_2$ for (i,j) next-nearest neighbors.

We study this model on two different two-dimensional lattices of $N=8$ sites, as shown in Fig. 1, with periodic

FIG. 1. Two two-dimensional eight-site lattices studied in this paper: (a) $L_x \times L_y = 4 \times 2$, and (b) a tilted square. t_x and t_y are the nearest-neighbor hoppings in x and y direction, and t_2 is the next-nearest-neighbor hopping.

boundary conditions. What we are investigating is the possibility of the appearance of superconductivity due to the Coulomb repulsion energy U, as suggested by several authors.[1-11] We define a complete set of pairing operators

$$\Delta_{\mathbf{a}} = \frac{1}{\sqrt{N}} \sum_{\mathbf{r}} C_{\mathbf{r}+\mathbf{a}\uparrow} C_{\mathbf{r}\downarrow} = \frac{1}{\sqrt{N}} \sum_{\mathbf{k}} e^{i\mathbf{k}\cdot\mathbf{a}} C_{\mathbf{k}\uparrow} C_{-\mathbf{k}\downarrow} \ . \tag{4}$$

where $\mathbf{a}$ is a displacement vector on the lattice. Using a linear combination of $\Delta_{\mathbf{a}}$'s, pair operators of various symmetries can be constructed. For example, operators with extended s-, d-, and p-wave symmetry involving only nearest-neighbor electrons have the form

$$\Delta_{s^*} = \Delta_{-\hat{x}} + \Delta_{\hat{x}} + \Delta_{-\hat{y}} + \Delta_{\hat{y}} \ , \tag{5}$$

$$\Delta_d = \Delta_{-\hat{x}} + \Delta_{\hat{x}} - \Delta_{-\hat{y}} - \Delta_{\hat{y}} \ , \tag{6}$$

and

$$\Delta_{p_x} = \Delta_{-\hat{x}} - \Delta_{\hat{x}} \ , \tag{7a}$$

$$\Delta_{p_y} = \Delta_{-\hat{y}} - \Delta_{\hat{y}} \ , \tag{7b}$$

respectively. We diagonalize an $N \times N$ pairing susceptibility matrix, defined by,

$$P_{\mathbf{ab}} = \int_0^\beta d\tau \langle \Delta_{\mathbf{a}}(\tau) \Delta_b^\dagger(0) \rangle \tag{8}$$

and study the behavior of its eigenvalues and eigenvectors as functions of the temperature and the Coulomb repulsion U. If superconductivity does exist in this model, the largest eigenvalue of $P_{\mathbf{ab}}$, corresponding to the susceptibility of the pairs described by its associated eigenvector, will diverge as the temperature goes to zero.

We calculate $P_{\mathbf{ab}}$ by diagonalizing the Hamiltonian and obtaining all the eigenvalues of H. For the eight-site Hubbard model the total Hilbert space is $4^8 = 65\,536$. Fortunately, we can use symmetries to reduce the dimensionality of matrices to be diagonalized. Three symmetries are used—the total particle number N_e, the total spin in the z direction S_z, and translational invariance. The biggest matrix in our calculation after using these symmetries is 628×628. Since we are interested in the low-temperature properties of $P_{\mathbf{ab}}$ we used a canonical ensemble. The pairing operator connects the $(N_e - 2)$-particle space, as well as the $(N_e + 2)$-particle space, to the N_e-particle space so the chemical potential μ which enters Eq. (1) was set by

$$\mu = \tfrac{1}{4}[E_0(N_e + 2) - E_0(N_e - 2)] \ . \tag{9}$$

Here $E_0(N)$ is the ground-state energy of N electrons. When $\beta\Delta \gg 1$, where

$$\Delta = E_0(N_e + 2) - E_0(N_e) - 2\mu$$
$$= E_0(N_e - 2) - E_0(N_e) + 2\mu \ ,$$

our calculation is essentially equivalent to the usual grand canonical one. For the noninteracting case ($U = 0$), the difference between the canonical ensemble and grand canonical ensemble is less than 2% when $\beta \geq 8$.

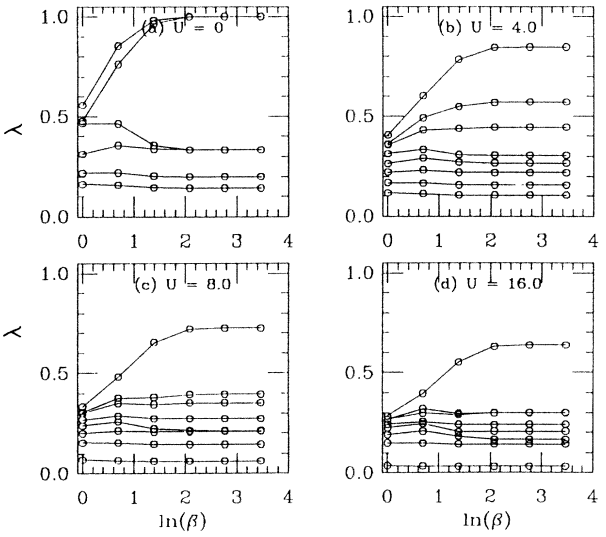

FIG. 2. All eigenvalues vs logarithm of the temperatures on a type-I (4×2) lattice with $N_e = 4$, $t_x = 1.0$, $t_y = 0.25$, and $t_2 = 0$ for (a) $U = 0$, (b) $U = 4$, (c) $U = 8$, and (d) $U = 16$.

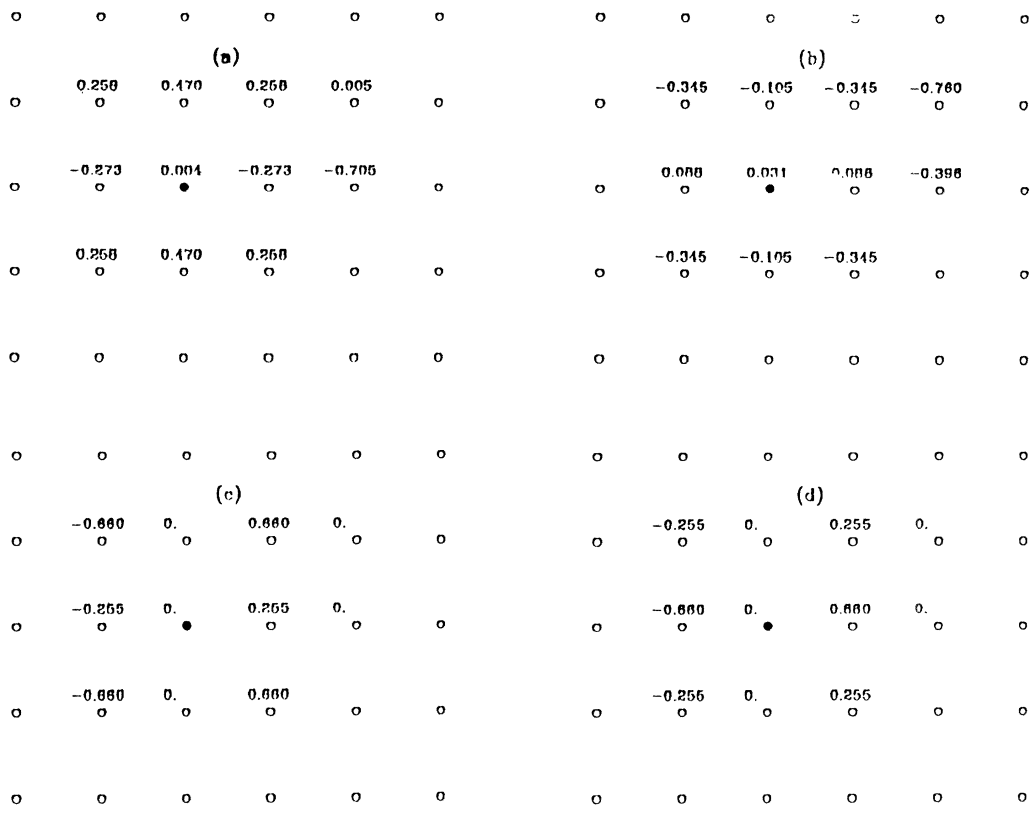

FIG. 3. Pairing structures of (a) the largest eigenvalue, (b) the second-largest eigenvalue, (c) the third-largest eigenvalue, and (d) the sixth-largest eigenvalue on a type-I (4×2) lattice with $N_e=4$, $t_x=1.0$, $t_y=0.25$, and $t_2=0$ for $U=16$, $\beta=32$.

III. NUMERICAL RESULTS

In this section we present numerical results for the eigenvalues of the pairing susceptibility matrix P_{ab} as functions of temperature T for various values of U. The pairing susceptibility matrix is positive definite, and its eigenvalues and eigenvectors depend on band filling and hoppings as well. We have concentrated on four cases, in the first three cases we use the type-I lattice (2×4), and in the last case we use the type-II lattice (tilted eight-site). Then all the eigenvalues λ are plotted versus $\ln(\beta)$ for given values of U (Figs. 2, 4, 6, and 8). The solid lines in the figures connect eigenvalues corresponding to the same eigenvector structure. Figures 3, 5, 7, and 9 show the structure of various eigenvectors. In the following we discuss each of the four cases.

Case (i)

$$N_e=4,\quad t_x=1.0,\quad t_y=0.25,\quad t_2=0\ .$$

In case (i) the largest eigenvalue first increases and then saturates as the temperature decreases to zero. The largest eigenvalue is a decreasing function of increasing Coulomb repulsion U at low temperature, and so are the other eigenvalues, as shown in Fig. 2. Four eigenvectors are plotted in Fig. 3 for $U=16$, $\beta=32$. The eigenvectors

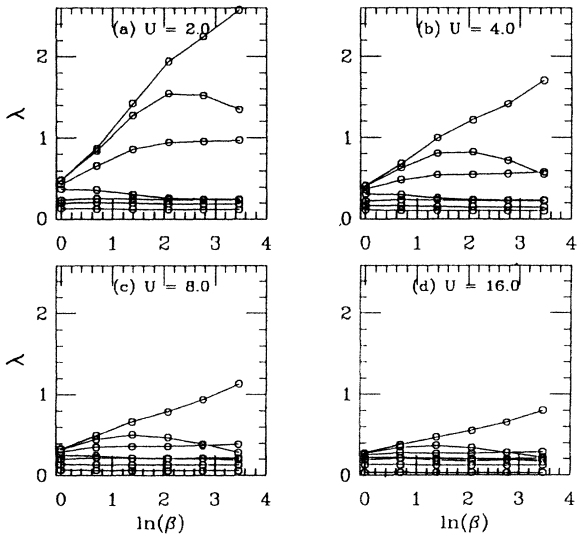

FIG. 4. All eigenvalues vs logarithm of the temperatures on a type-I (4×2) lattice with $N_e=4$, $t_x=1.0$, $t_y=0.50$, and $t_2=0$ for (a) $U=2$, (b) $U=4$, (c) $U=8$, and (d) $U=16$. There are two identical eigenvalues in this case.

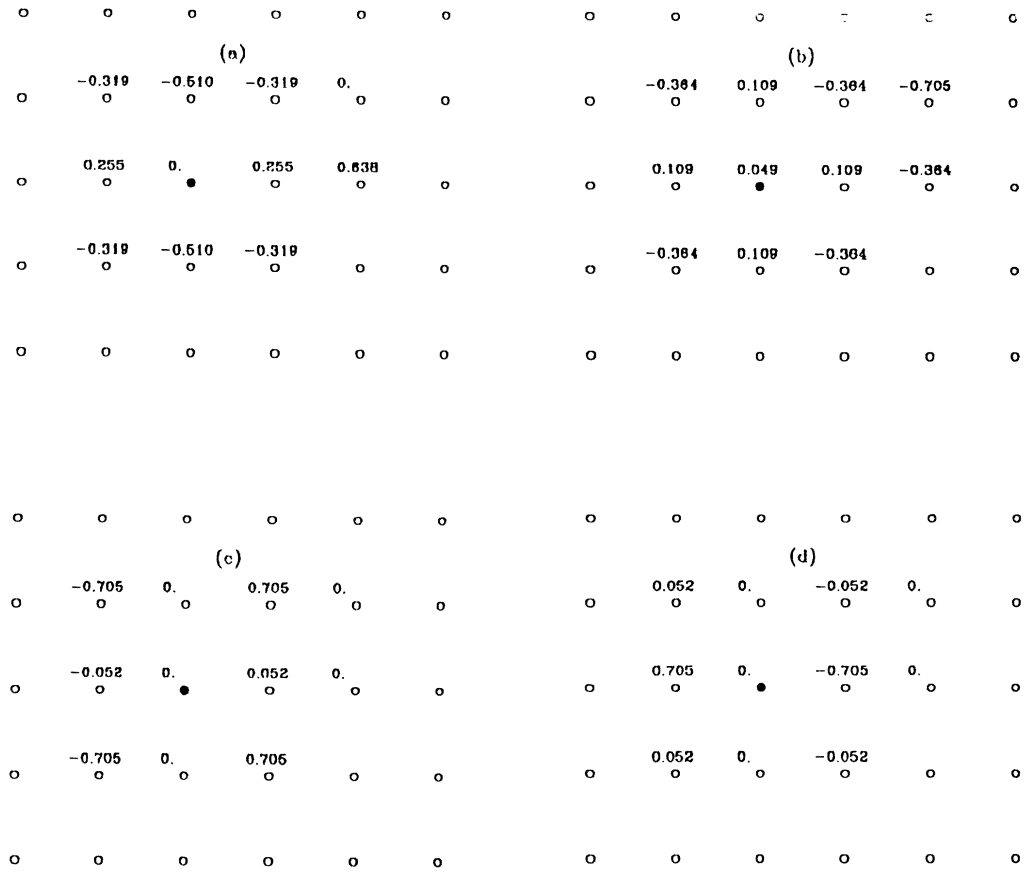

FIG. 5. Pairing structure of (a) the largest eigenvalue, (b) the second-largest eigenvalue, (c) the third-largest eigenvalue, and (d) the sixth-largest eigenvalue on a type-I (4×2) lattice with $N_e=4$, $t_x=1.0$, $t_y=0.50$, and $t_2=0$ for $U=16$, $\beta=32$.

of the first- and second-largest eigenvalues shown in Figs. 2(a) and 2(b) have mixed *s*- and *d*-wave symmetry. The eigenvectors of the third- and sixth-largest eigenvalue shown in Figs. 2(c) and 2(d) are *p*-wave-like. Note that the amplitude at the origin is always very small, due to the large on-site repulsion and that one also gets appreciable amplitudes beyond nearest neighbors. For the noninteracting case, the amplitudes at all sites are found to be identical for the eigenvector with the largest eigenvalue.

Case (ii)

$$N_e=4,\quad t_x=1.0,\quad t_y=0.50,\quad t_2=0\ .$$

This case differs from case (i) since the largest eigenvalue does not saturate as the temperature goes to zero. This is due to the degeneracy at the Fermi energy when $U=0$. Such unphysical degeneracy comes from the finiteness of the small cluster and can be avoided if one turns on the next-nearest-neighbor hopping t_2. For $t_2\neq0$, we find that the largest eigenvalue saturates as $T\rightarrow0$ (we do not show the results here). Here again all eigenvalues are suppressed by U, as one can see from Fig. 4. The pairing structure corresponding to the largest eigenvalue Fig. 5(a) again has mixed *s*-*d* symmetry while the structure of the second-largest eigenvalue is an ex-

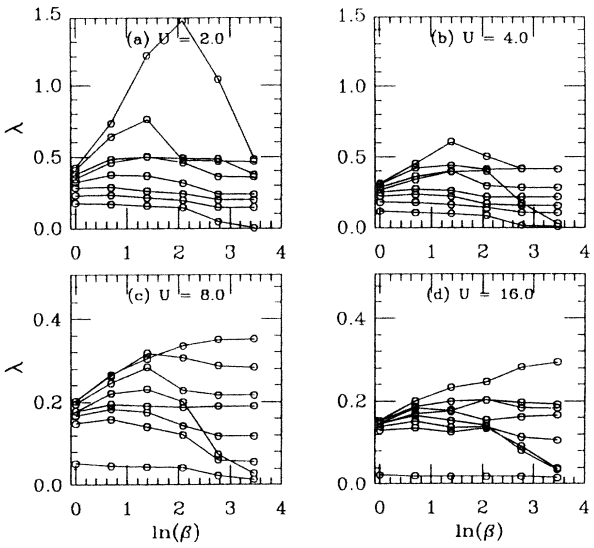

FIG. 6. All eigenvalues vs logarithm of the temperatures on a type-I (4×2) lattice with $N_e=6$, $t_x=1.0$, $t_y=0.25$, and $t_2=0$ for (a) $U=2$, (b) $U=4$, (c) $U=8$, and (d) $U=16$. Note the different scales used for (a), (b), and (c), (d).

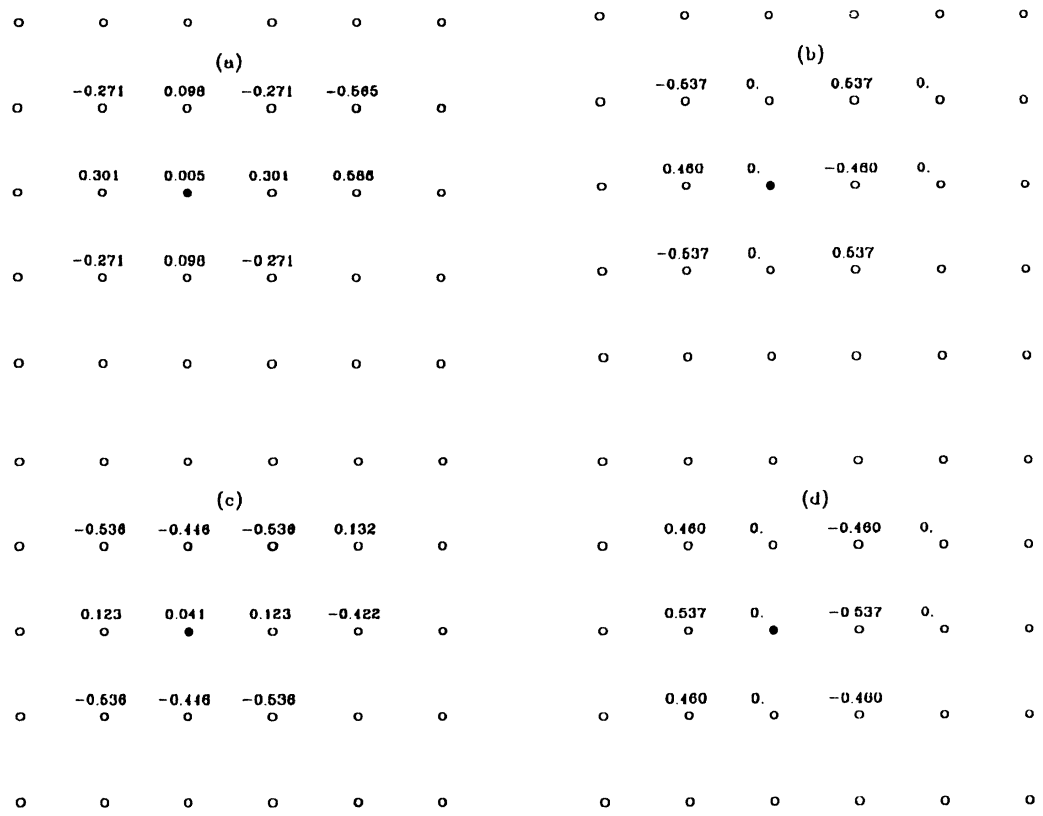

FIG. 7. Pairing structures of (a) the largest eigenvalue, (b) the second-largest eigenvalue, (c) the third-largest eigenvalue, and (d) the seventh-largest eigenvalue on a type-I (4×2) lattice with $N_e=6$, $t_x=1.0$, $t_y=0.25$, and $t_2=0$ for $U=16$, $\beta=32$.

tended s wave [Fig. 5(b)]. The structure of the eigenvectors of the third- and sixth-largest eigenvalues are also shown.

Case (iii)

$$N_e=6,\quad t_x=1.0,\quad t_y=0.25,\quad t_2=0\ .$$

Here the band filling is $\rho=0.75$, and the results for the eigenvalues and eigenvectors are shown in Figs. 6 and 7. For small U, some of the eigenvalues show a peak and do not vary with temperature monotonically. The eigenvector of the largest eigenvalue looks like an extended s wave and that of the second-largest eigenvalue has p_x-wave symmetry. d-wave pairing is now the third-largest eigenvalue. Note that the eigenvalues are decreasing functions of U as before.

The final case we will consider corresponds to a type-II lattice (tilted eight-site):

Case (iv)

$$N_e=4,\quad t_x=t_y=1.0,\quad t_2=0.125\ .$$

As previously discussed, we have set $t_2\neq0$ in order to remove the degeneracy at the Fermi surface when $U=0$. The structures of the pairing eigenvectors shown in Fig. 9 for $U=16$ and $\beta=32$ are simpler than in the other three cases. The eigenvalues show peaks at intermediate temperatures, and the largest eigenvalue drops as the temper-

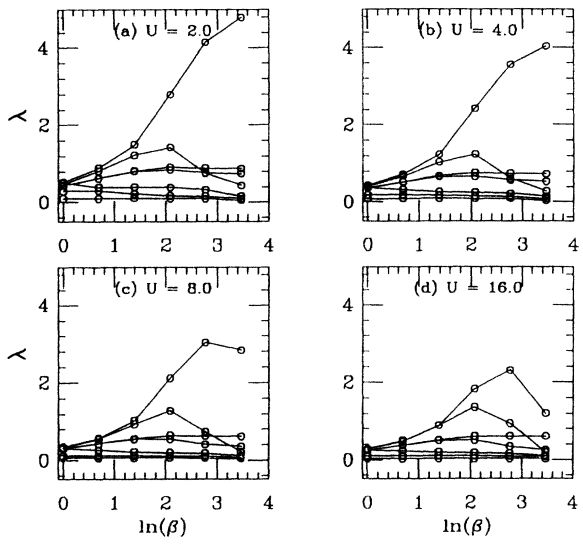

FIG. 8. All eigenvalues vs logarithm of the temperatures for the type-II (tilted square) lattice with $N_e=4$, $t_x=t_y=1.0$, and $t_2=0.125$ for (a) $U=2$, (b) $U=4$, (c) $U=8$, and (d) $U=16$. There are two identical eigenvalues in this case.

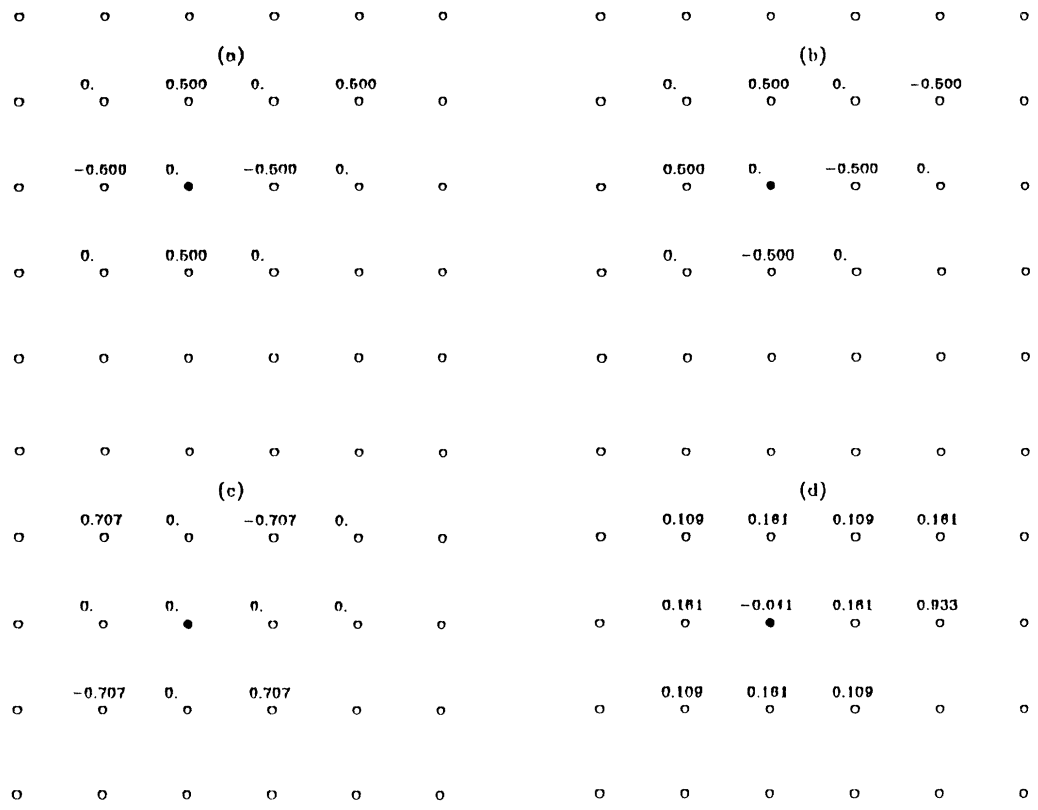

FIG. 9. Pairing structures of (a) the largest eigenvalue, (b) the second- and third-largest eigenvalues, (c) the fourth-largest eigenvalue, and (d) the fifth-largest eigenvalue for the type-II (tilted square) lattice with $N_e=4$, $t_x=t_y=1.0$, and $t_2=0.125$ for $U=16$, $\beta=32$.

ature approaches zero (Fig. 8). As seen from Fig. 9, the eigenvector of the largest eigenvalue is a d wave, and the eigenvectors of the second- and third-largest eigenvalues are p waves involving only nearest-neighbor sites. The eigenvector of the fourth-largest eigenvalue is d wave involving next-nearest-neighbor sites only, and the rest are extended s waves. Just as in the previous three cases, the largest eigenvalue decreases as U increases. These results clearly show that the Coulomb repulsion U suppresses the pairing susceptibilities of the most stable pairing structure regardless of what kind of symmetry it has.

As a further check on our procedure, we have performed the calculation for negative values of U and always found strong enhancement of the susceptibility corresponding to the largest eigenvalue compared with the noninteracting case, as expected. An example is shown in Fig. 10, for case (i), and the structure of the pairing eigenvectors is shown in Fig. 11.

IV. PERTURBATION THEORY

We have also investigated the various pairing susceptibilities using perturbation theory. As discussed in Ref. 14, perturbation theory can provide useful insight at higher temperatures and moderate U values.

In particular, here we are interested in determining whether the leading contributions of the interaction to the pair susceptibility enhance or reduce it. Consider, for example, the d-wave pair susceptibility

$$P_d=\int_0^\beta d\tau\langle\Delta_d(\tau)\Delta_d^\dagger(0)\rangle \tag{10}$$

with Δ_d given by Eq. (6) of Sec. II. Fourier transforming the site-operator expression gives

$$\Delta_d=\sum_p g(p)C_{p\uparrow}C_{-p\downarrow} \tag{11}$$

with the form factor

$$g(p)=\cos p_x-\cos p_y\ . \tag{12}$$

For a noninteracting system

$$P_d^{(0)}=\frac{T}{N}\sum_{p,n}\frac{g^2(p)}{\omega_n^2+\varepsilon_p^2}$$
$$=\frac{1}{N}\sum_p\frac{\tanh(\beta\varepsilon_p/2)}{2\varepsilon_p}(\cos^2p_x+\cos^2p_y)\ . \tag{13}$$

If $t_2=\mu=0$ one finds

$$P_d^{(0)}=\frac{1}{4\pi^2t}\left[\ln^2\left[\frac{2t}{T}\right]+2\ln\left[\frac{16\gamma}{\pi}\right]\ln\left[\frac{2t}{T}\right]+c\right] \tag{14}$$

with $c=2.13$. Here, the $\ln^2(2t/T)$ term arises from the overlap of the Van Hove singularity in the density of

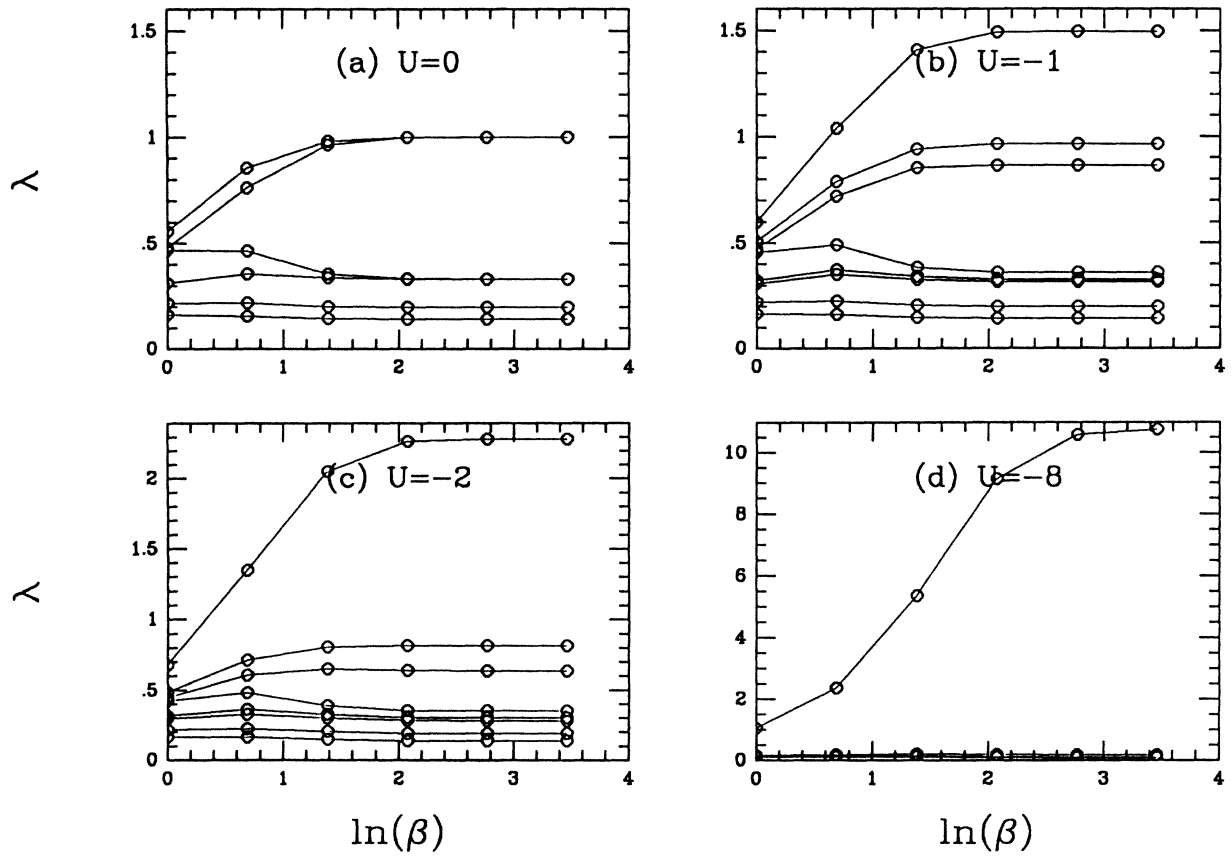

FIG. 10. All eigenvalues vs logarithm of the temperature on a type-I (4×2) lattice with $N_e=4$, $t_x=1.0$, $t_y=0.25$, and $t_2=0$ for (a) $U=0$, (b) $U=-1$, (c) $U=-2$, and (d) $U=-8$.

states with the usual BCS $\ln(2t/T)$ term. More generally,[14] if $t_2\neq 0$ the perfect nesting of the Fermi surface is destroyed, but if $\mu=-4t_2$ the leading behavior of $P_d^{(0)}$ remains $\ln^2(2t/T)$ with the coefficient in Eq. (13) multiplied by

$$\left[1-\left[\frac{2t_2}{t}\right]^2\right]^{-1/2}.$$

As μ moves away from $4t_2$, the leading behavior of $P_d^{(0)}$ changes to the usual $N(\mu)\ln(2t/T)$ form, where $N(\mu)$ is the density of states at the Fermi surface.

The leading contributions from the interaction are shown in Fig. 12. The vertex corresponds to the form factor $g(p)$. To linear order in U, Fig. 12(a) gives

$$P_d^{(1)}=-U\left[\frac{T}{N}\right]^2\sum_{p,n}\sum_{p',n'}\frac{g(p)}{\omega_n^2+\varepsilon_p^2}\frac{g(p')}{\omega_{n'}^2+\varepsilon_{p'}^2}. \tag{15}$$

For $g(p)=\cos p_x-\cos p_y$, the sum vanishes

$$\sum_p\frac{g(p)}{\omega_n^2+\varepsilon_p^2}=0 \tag{16}$$

so that for the d wave, the pair field is not reduced by the linear U term. The second-order terms, Figs. 12(b) and 12(c), correspond to the leading contributions from the interaction and self-energy, respectively. The latter self-energy part is twice the contribution of the diagram shown in Fig. 12(c), since either propagator can be dressed. From Eq. (16) it follows that the second-order ladder contribution vanishes.

The interaction Fig. 12(b) gives a positive contribution and enhances the pairing susceptibility. It is just the leading term in the RPA spin-fluctuation-mediated Berk-Schrieffer[15] interaction. However, the self-energy terms give a negative contribution and suppress the pair susceptibility. We have numerically evaluated the diagrams in Figs. 12(b) and 12(c) for a range of β. Figure 13 shows $(P_b+2P_c)/U^2$ versus β for various values of the chemical potential μ. Here P_b is the contribution from the diagram in Fig. 12(b), and $2P_c$ is twice the contribution of the diagram in Fig. 12(c) divided. Now to the leading order in the interaction we have

$$P_d=P_d^{(0)}+(P_b+2P_c), \tag{17}$$

and from Fig. 13 we see that the effect of U is to *reduce* the d-wave pairing susceptibility for a range of temperatures. As μ decreases and the system moves away from the region of large spin-density wave fluctuations, the temperature at which (P_b+2P_c) becomes positive in-

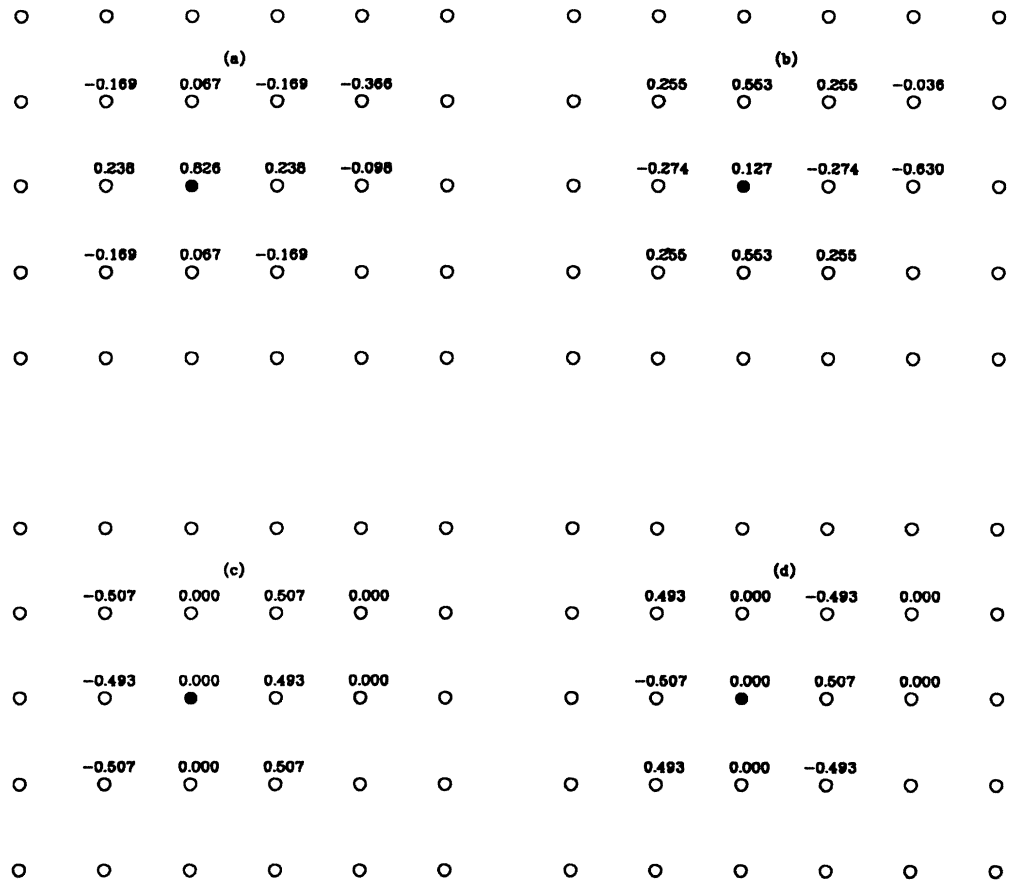

FIG. 11. Pairing structures of (a) the largest eigenvalue, (b) the second-largest eigenvalue, (c) the third-largest eigenvalues, and (d) the fourth-largest eigenvalue for the case of Fig. 10(b) ($U=-1$) for $\beta=32$.

creases. However, as this happens the size of the spin-fluctuation contribution decreases and the pairing interaction becomes weak.[16] Naturally, for a given value of U, as the temperature decreases, higher-order terms become important, and perturbation theory fails. Nevertheless, the fact that the leading-order term suppresses the pairing over a wide region of temperature is quite different from the case of the electron-phonon interaction or the behavior of χ for a Heisenberg ferromagnet as J is increased.

V. DISCUSSION

We have presented numerical results for pairing susceptibilities on eight-site Hubbard clusters. The results for such small systems are naturally very sensitive to the geometry, boundary conditions, and relative size of the hopping parameters. Nevertheless, in studying several different cases we have consistently found suppression of all pairing susceptibilities by the Hubbard repulsion. Our calculation took into account all possible pair wave func-

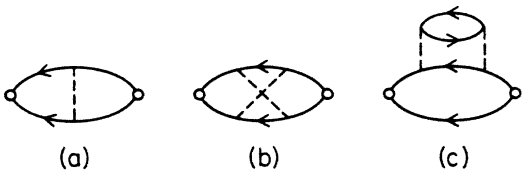

FIG. 12. Perturbation theory graphs for the d-wave pairing susceptibility (a) lowest order, (b) second-order interaction, (c) second-order self-energy. The vertices on each end of a graph correspond to the form factor $g(p)$.

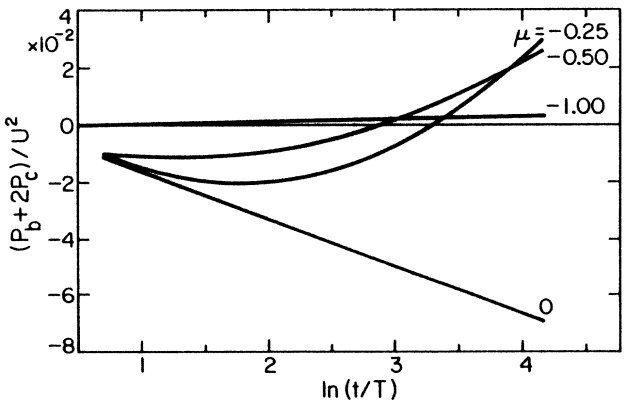

FIG. 13. The leading correction to the pairing susceptibility obtained from the graphs shown in Figs. 10(b) and 10(c), $(P_b+2P_c)/v^2$ vs $\ln(t/T)$ for various values of the chemical potential μ. Here μ is measured in units where $t=1$.

tions that fit onto the clusters considered.

Our results are in contradiction with expectations that in the presence of U the resulting superexchange interaction would induce superconductivity. In the presence of U, the electron pairs associated with the largest pairing susceptibility tend to rearrange themselves so that the weight of the pair wave function at the origin is small. This rearrangement of the wave function to avoid double occupancy evidently causes suppression of the pairing susceptibility in these small systems, and we expect this to carry over to large systems. Emery has suggested that this should occur in a one-band model but not in a two-band model.[17]

Our perturbation theory results also give some insight into why RPA-like calculations fail. The lowest-order self-energy diagram is larger and of opposite sign than the corresponding one for the effective interaction, yielding a net suppression of pairing. In third order we have found vertex corrections which also suppress pairing.

Our results here, together with recent Monte Carlo results,[12] suggests that the 2D Hubbard model does not exhibit superconductivity. This does not, however, necessarily rule out spin fluctuations as playing a role in high-T_c superconductivity, for example, in a two-band model[17,18] or with phonons also playing an essential role.[19] We can also not rule our superconductivity in the 2D Hubbard model at very low temperatures involving very extended pair states, although this would probably not be relevant for high T_c.

ACKNOWLEDGMENTS

This work was supported by the National Science Foundation under Grant Nos. DMR-85-17756, (H.Q.L., J.E.H.) and DMR-86-15454 (D.J.S.). Computations were performed at the Cray X-MP of the San Diego Supercomputer Center. J.H. is grateful to Cray Corporation and AT&T Bell Laboratories for financial support.

*Present address: Department of Physics, 510A Brookhaven National Laboratory, Upton, N.Y. 11973.

[1]P. W. Anderson, Science **235**, 1196 (1987).
[2]J. E. Hirsch, Phys. Rev. Lett. **54**, 1317 (1985).
[3]D. J. Scalapino, E. Loh, and J. E. Hirsch, Phys. Rev. B **34**, 8190 (1986).
[4]J. Miyake, S. Schmitt-Rink, and C. Varma, Phys. Rev. B **34**, 6554 (1986).
[5]G. Baskaran, Z. Zou, and P. W. Anderson, Solid State Commun. **63**, 973 (1987).
[6]A. Ruckenstein, P. Hirschfield, and J. Appel, Phys. Rev. B **36**, 857 (1987).
[7]C. Gros, R. Joynt, and T. M. Rice (unpublished).
[8]M. Cyrot, Solid State Commun. **62**, 821 (1987).
[9]H. J. Schulz (unpublished).
[10]F. J. Ohkawa, J. Phys. Soc. Jpn. (to be published).
[11]N. E. Bickers, D. J. Scalapino, and R. T. Scalettar (unpublished).
[12]J. E. Hirsch and H. Q. Lin, Phys. Rev. B (to be published).
[13]G. Kotliar (unpublished).
[14]J. E. Hirsch and D. J. Scalapino, Phys. Rev. Lett. **56**, 2732 (1986).
[15]N. F. Berk and J. R. Schrieffer, Phys. Rev. Lett. **17**, 433 (1986).
[16]See the results for the λ_d given in Ref. 11.
[17]V. J. Emery, Phys. Rev. Lett. **58**, 2794 (1987).
[18]J. E. Hirsch, Phys. Rev. Lett. **59**, 228 (1987).
[19]J. E. Hirsch, Phys. Rev. B **35**, 8726 (1987).